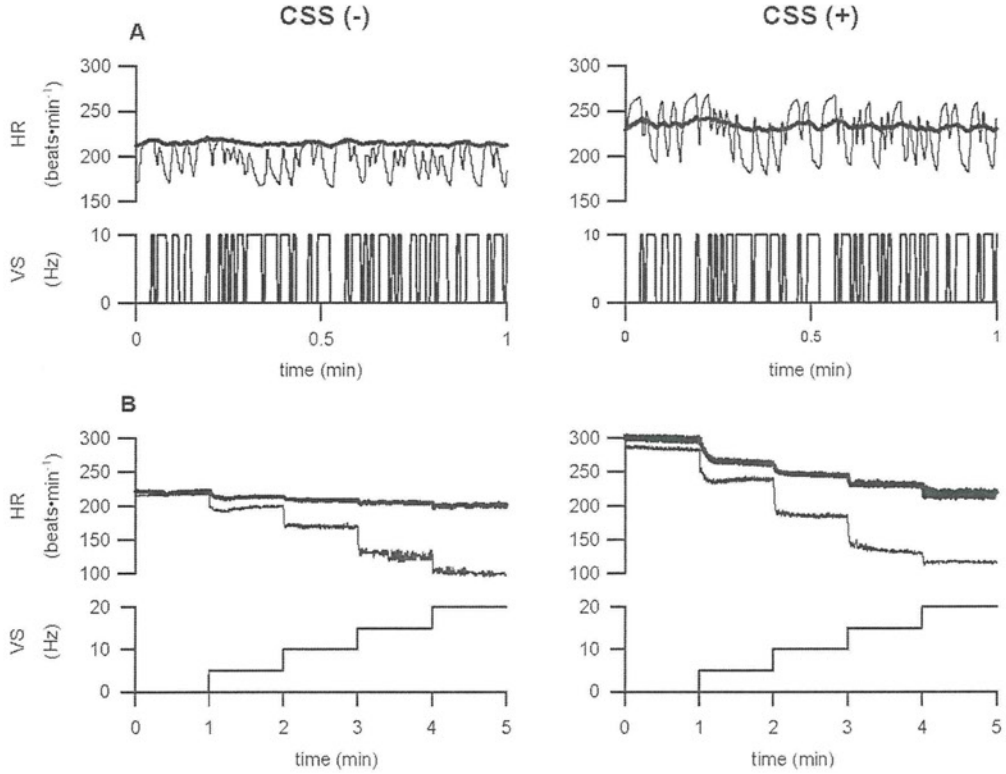

Fig. 1. A: Representative recordings of HR obtained utilizing binary white-noise vagal stimulation (top) and the corresponding vagal stimulation (VS; bottom) without (left) and with (right) CSS. Thin line, control; thick line, K_{ACh} channel blockade with tertiapin (30 nmol·kg^{-1} iv). **B**: Representative recordings of HR obtained utilizing stepwise vagal stimulation (top) and the corresponding VS (bottom) without (left) and with (right) CSS, which increased the basal HR and the amplitude of HR variation in both binary white-noise and stepwise vagal stimulations. A K_{ACh} channel blockade attenuated the amplitude of HR variation and the speed of the response of HR to vagal stimulation regardless of CSS.

Table 1. Effects of tertiapin infusion and CSS on AP and HR before and during dynamic vagal stimulation.

	CSS (–)		CSS (+)		Comparison factors		
	Control	Tertiapin	Control	Tertiapin	Drug	CSS	Interaction
AP, mmHg							
Before stimulation	82.2 ± 16.8	76.7 ± 20.1	90.5 ± 13.8	81.8 ± 16.6	0.022	0.641	0.546
During stimulation	80.2 ± 18.4	76.6 ± 21.4	81.8 ± 14.8	75.9 ± 19.0	0.144	0.962	0.709
HR, beats·min^{-1}							
Before stimulation	247.8 ± 20.1	247.9 ± 30.8	312.2 ± 15.6	307.4 ± 20.9	0.521	<0.001	0.494
During stimulation	211.9 ± 17.5**	228.3 ± 23.4	244.3 ± 33.3**	248.1 ± 30.7**	0.026	<0.001	0.308

Values are means ± SD (n = 7). CSS, cardiac sympathetic stimulation; AP, arterial pressure; HR, heart rate. **P < 0.01 vs. corresponding values before stimulation. Tertiapin was infused at 30 nmol/kg iv.

input signal and not the vagal stimulation frequency itself. Table 2 summarizes parameters of the transfer function at 0.01, 0.1, 0.5, and 1 Hz and also those of the step response. Tertiapin attenuated the dynamic gain compared with the control conditions regardless of CSS. The phase approached –Π radians at the lowest frequency and lagged with increasing frequency under the control conditions. Tertiapin increased the phase delay in the frequency range from 0.01 to 1 Hz. Coherence was near unity in the overall frequency range under the control conditions. A decrease in the coherence function from unity was noted >0.6 Hz under the condition of the K_{ACh} channel blockade, which was reversed by CSS.

Figure 2B shows the calculated step response of HR to vagal stimulation averaged for all animals under the conditions of control (thin lines) and K_{ACh} channel blockade

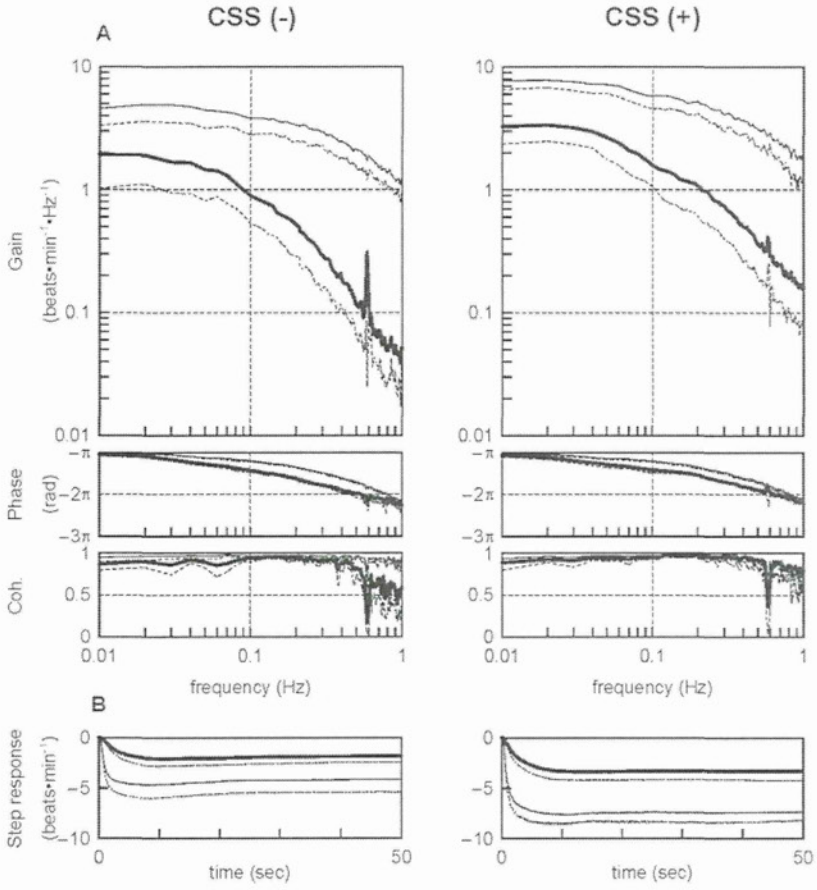

Fig. 2. A: Dynamic transfer function relating vagal stimulation to the HR responses averaged from all animals (pooled data; n = 7) without (left) and with (right) CSS. Solid lines, means; dashed lines, –SD. Thin line, control; thick line, a K_{ACh} channel blockade with tertiapin (30 nmol·kg^{-1} iv). Top: gains; middle: phase shifts; bottom: coherence (Coh) functions. Tertiapin decreased transfer gain and increased the phase shift with increasing frequency. Cardiac sympathetic stimulation increased transfer gain both under control conditions and under conditions of a K_{ACh} channel blockade without affecting the phase shift. **B**: Calculated step response to 1 Hz tonic vagal stimulation averaged from all animals (pooled data; n = 7) without (left) and with (right) CSS. Solid lines, means; dashed lines, –SD. Thin line, control; thick line, K_{ACh} channel blockade with tertiapin (30 nmol·kg^{-1} iv). The K_{ACh} channel blockade decreased the maximum step response and slowed the initial step response. CSS increased the maximum step response both under control conditions and under conditions of a K_{ACh} channel blockade without affecting the initial response (see Table 2).

Table 2. Effects of tertiapin infusion and CSS on parameters of the transfer function and step response.

	CSS (–)		CSS (+)		Comparison factors		
	Control	Tertiapin	Control	Tertiapin	Drug	CSS	Interaction
Gain, beats·min^{-1}·Hz^{-1}							
0.01 Hz	4.58 ± 1.26	2.21 ± 0.97	7.73 ± 1.15	3.28 ± 0.92	<0.001	0.001	0.007
0.1 Hz	3.81 ± 1.01	1.10 ± 0.43	5.82 ± 1.28	1.60 ± 0.54	<0.001	0.007	0.015
0.5 Hz	2.12 ± 0.64	0.16 ± 0.07	3.08 ± 0.82	0.36 ± 0.17	<0.001	0.013	0.081
1 Hz	1.09 ± 0.27	0.08 ± 0.03	1.73 ± 0.61	0.16 ± 0.08	<0.001	0.019	0.044
Phase, rad							
0.01 Hz	3.10 ± 0.04	2.99 ± 0.11	2.99 ± 0.11	2.92 ± 0.14	0.037	0.077	0.579
0.1 Hz	2.52 ± 0.08	1.78 ± 0.17	2.52 ± 0.11	1.83 ± 0.25	<0.001	0.757	0.719
0.5 Hz	0.91 ± 0.13	0.03 ± 0.27	0.90 ± 0.10	0.35 ± 0.10	<0.001	0.011	0.056
1 Hz	–0.56 ± 0.33	–0.81 ± 0.21	–0.41 ± 0.26	–0.64 ± 0.18	0.014	0.159	0.905
Coherence							
0.01 Hz	0.95 ± 0.05	0.87 ± 0.07	0.93 ± 0.04	0.89 ± 0.09	0.005	0.947	0.424
0.1 Hz	0.96 ± 0.03	0.94 ± 0.04	0.97 ± 0.01	0.95 ± 0.02	0.004	0.440	0.835
0.5 Hz	0.96 ± 0.02	0.83 ± 0.08	0.91 ± 0.08	0.93 ± 0.04	0.026	0.259	0.006
1 Hz	0.90 ± 0.07	0.59 ± 0.16	0.78 ± 0.15	0.79 ± 0.12	0.017	0.312	0.011
Maximum step response, beats·min^{-1}	–4.2 ± 1.2	–1.8 ± 0.6	–7.4 ± 0.9	–3.3 ± 0.9	<0.001	<0.001	0.005
Time constant, s	0.63 ± 0.09	3.34 ± 0.55	0.74 ± 0.18	3.18 ± 1.10	<0.001	0.913	0.560

Values are means ± SD (n = 7). CSS, cardiac sympathetic stimulation. Tertiapin was infused at 30 nmol/kg iv.

Table 3. Effects of tertiapin infusion and CSS on parameters of the transfer function relating dynamic vagal stimulation to HR.

	CSS (–)		CSS (+)		Comparison factors		
	Control	Tertiapin	Control	Tertiapin	Drug	CSS	Interaction
Dynamic gain, beats·min^{-1}·Hz^{-1}	4.6 ± 1.1	2.3 ± 0.9	7.3 ± 1.1	3.6 ± 1.0	<0.001	<0.001	0.037
Corner frequency, Hz	0.26 ± 0.04	0.05 ± 0.01	0.23 ± 0.06	0.06 ± 0.02	<0.001	0.439	0.1613
Lag time, s	0.38 ± 0.04	0.45 ± 0.04	0.34 ± 0.04	0.38 ± 0.03	<0.001	0.002	0.2776

Values are means ± SD (n = 7). CSS, cardiac sympathetic stimulation; HR, heart rate. Tertiapin was infused at 30 nmol/kg iv.

(thick lines), without (left) and with (right) CSS. Tertiapin slowed the transient response and attenuated the HR response to vagal stimulation in the time domain. CSS did not affect the time constant, though it augmented the maximum step response. A significant interaction was observed between the tertiapin and CSS effects in the maximum step response, but not in the time constant (Table 2).

The fitted parameters of the transfer functions are summarized in Table 3. Tertiapin significantly decreased the dynamic gain and the corner frequency and significantly increased the lag time. Conversely, CSS significantly increased the dynamic gain and significantly decreased the lag time. A significant interaction was observed between the tertiapin and CSS effects only in dynamic gain.

Static protocol

Figure 3A summarizes changes in HR in response to stepwise vagal stimulation without (left) and with (right) CSS, which increased basal HR obtained at 0 Hz vagal stimulation by approximately 50 beats·min^{-1}. Tertiapin significantly attenuated the bradycardic response to vagal stimulation regardless of CSS. The magnitude of attenuation (i.e., the difference between the open and closed symbols) became greater as the vagal stimulation frequency increased.

Figure 3B demonstrates the HR reduction obtained under four conditions at each frequency. To aid an intuitive understanding, the tertiapin condition is designated as D(–) in this panel because tertiapin blocked the direct action of ACh. S(+) indicates the presence of CSS. At 5 Hz vagal stimulation frequency, the direct action alone S(–)D(+) significantly augmented the HR reduction, as depicted by the diagonal hatch. CSS alone S(+)D(–) also significantly augmented the HR reduction, as depicted by the vertical hatch. The augmentation of the HR reduction obtained by S(+)D(+) exceeded the simple summation of the diagonal hatch and vertical hatch, suggesting that the effect of the direct action was enhanced by CSS (depicted in the solid rectangle). The positive interaction waned at 10 Hz vagal stimulation and disappeared at 15 and 20 Hz vagal stimulation. That is, the simple summation of the diagonal hatch and vertical hatch largely explained the augmentation of the HR reduction attained by S(+)D(+) at 15 and 20 Hz vagal stimulation.

DISCUSSION

We have examined the effect of background sympathetic tone on the direct action of ACh through K_{ACh} channels by examining the dynamic and static transfer characteristics. The major findings in the present study are that the bradycardic response to vagal stimulation via the K_{ACh} channels was augmented by concomitant CSS, depending on vagal stimulation frequency. The rapidity of vagal HR control obtained by the K_{ACh} channels, however, was not affected by CSS. These findings support our hypotheses and demonstrated, for the first time to our knowledge, the existence of an accentuated antagonism in the direct action of ACh through the K_{ACh} channels.

Effect of CSS on the rapidity of vagal HR control via K_{ACh} channels

Our results indicate that the rapidity of the vagal HR control via the K_{ACh} channels was not affected by background sympathetic tone. In the transfer function, the phase values were significantly more delayed by the K_{ACh} channel blockade in the frequency range from 0.01 to 1 Hz in agreement with our previous study [6]. In contrast, CSS did not affect the phase characteristics, in which no significant interaction was observed at each frequency (Table 2). Moreover, the calculated step response clearly demonstrated that tertiapin significantly prolonged the time constant by >2 s, whereas CSS did not affect it (Fig. 2B and Table 2).

Changes in fitted parameters of the transfer function from vagal stimulation to HR also support our first hypothesis that CSS does not affect the rapidity of the vagal HR control mediated by the K_{ACh} channels. Tertiapin decreased the corner frequency to a similar degree without or with CSS, which did not affect the corner frequency. On the other hand, tertiapin prolonged the lag time, whereas CSS shortened it (Table 3). However, changes in the lag time caused by tertiapin or CSS were less than 0.1 s and might

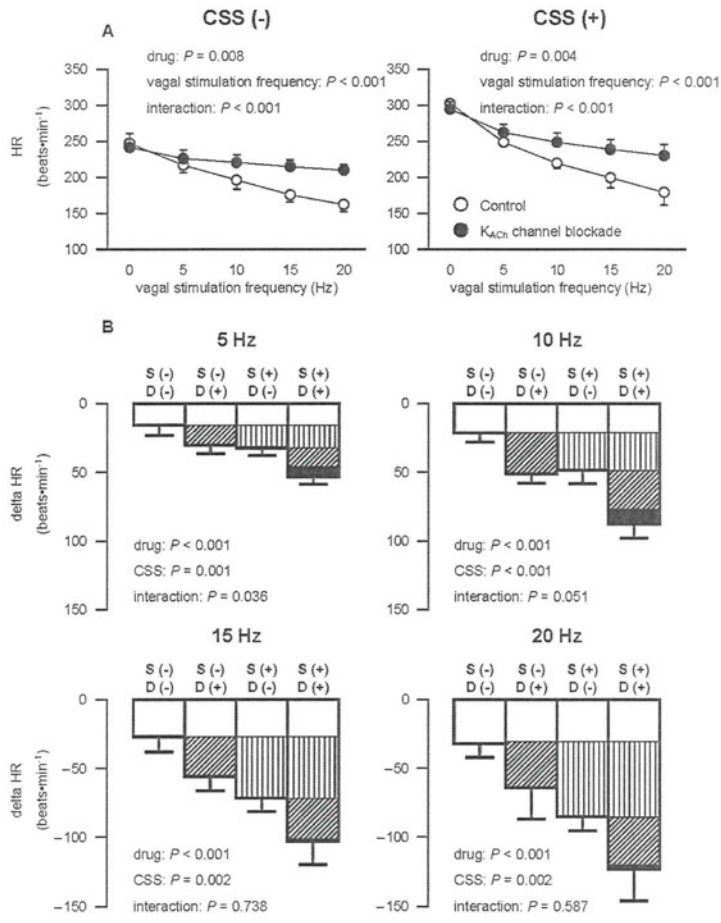

Fig. 3. A: Static HR responses relating stepwise vagal stimulation averaged from all animals (pooled data; n = 5) without (left) and with (right) CSS. A K_{ACh} channel blockade decreases the static HR response, and the static reductions in the bradycardic effect were greater at higher stimulation frequencies in both conditions. **B**: Changes in HR responses from baseline to vagal stimulation at 5 Hz (top left), 10 Hz (top right), 15 Hz (bottom left), and 20 Hz (bottom right) averaged from all animals (pooled data; n = 5). To aid an intuitive understanding, the tertiapin condition was designated as D(–) in this panel because tertiapin blocked the direct action of ACh. S(+) indicates the presence of CSS. Significant interaction and a tendency towards significant interaction (P = 0.051) were obtained at 5 and 10 Hz vagal stimulation, respectively, but not at 15 and 20 Hz vagal stimulation.

be insignificant in terms of physiological HR control.

Effect of CSS on the gain of vagal HR control via K_{ACh} channels

Because the direct action of ACh via K_{ACh} is considered to be independent of sympathetic control [12], an accentuated antagonism is unlikely to occur in the direct action. However, because the interbeat interval is determined by the pacemaker potential of the sinus node cells, which in turn depends on all of the potassium, sodium, and calcium currents, there could be interaction between the K_{ACh} channel pathway and background sympathetic tone when we observe the HR response. Changes in the sodium current and/or calcium current induced by background sympathetic tone would modify the effect of changes in the potassium current through the K_{ACh} channels.

Our results indicate that accentuated antagonism occurred, affecting the direct action of ACh in the range of mild vagal stimulation as follows. In the dynamic protocol that was carried out with a mean vagal stimulation frequency of 5 Hz, significant positive interaction was observed between the tertiapin and CSS effects, affecting the dynamic gain as well as the calculated maximum step response (Table 2), suggesting that the effect of the K_{ACh} channel pathway was enhanced during CSS. The static protocol also showed significant positive interaction at 5 Hz vagal stimulation (Fig. 3B). The augmentation of the bradycardic response to vagal stimulation gained by the direct action of ACh through the K_{ACh} channels was enhanced under concomitant CSS.

The reason for the absence of a positive interaction between the tertiapin and CSS effects at 15 and 20 Hz vagal stimulation is unclear (Fig. 3B). One possible explanation is the curvilinearity of the HR response to vagal stimulation. In the right panel of Fig. 3A, the tertiapin-free control data (open symbols), which correspond to S(+)D(+) in Fig. 3B, showed the steepest slope at the 0–5 Hz vagal stimulation step. The slope became shallower as the vagal stimulation frequency increased, suggesting a saturation phenomenon of HR reduction in response to vagal stimulation. It is very likely that such curvilinearity masked possible positive interaction between CSS and the direct action of ACh in determining the HR reduction during 15 and 20 Hz vagal stimulation. Accentuated antagonism in the direct action of ACh through K_{ACh} channels might therefore operate under balanced conditions of sympa-

thetic and vagal nerve activities.

The existence of an accentuated antagonism in the direct action of ACh through the K_{ACh} channels could be explained by macromolecular signaling complexes in which G protein-gated inwardly rectifying potassium (GIRK) channels are physically associated with signaling partner regulated by different G protein-coupled receptors (GPCRs) [19, 20]. Cardiac sympathetic stimulation simultaneously activates several different GPCRs: α-adrenergic, β1-adrenergic, and β2-adrenergic receptors. Notably, the β1-adrenergic receptor is coupled to downstream kinase, protein kinase A (PKA). The β-adrenergic signaling via PKA phosphorylation increases the activity of K_{ACh} channels [21, 22]. Taken together, β-adrenergic receptors might augment the activity of K_{ACh} channels via a PKA-dependent mechanism.

Limitations

This study has several limitations. First, the data was obtained from anesthetized animals. Since anesthesia would affect the autonomic tone, the results may not be directly applicable to conscious animals. However, because we cut and stimulated the right cardiac sympathetic and vagal nerves, changes in autonomic outflow associated with anesthesia might not have significantly affected the present results.

Second, we blocked the K_{ACh} channels to examine the effect of background sympathetic tone on the direct effect of ACh through the K_{ACh} channels. On the other hand, if we had blocked the indirect effect of ACh through the cyclic AMP pathway, leaving the direct effect of ACh intact, and then examined the effect of background sympathetic tone on the HR response to vagal stimulation, the results might have been excessively straightforward. However, we could find no blocker for the indirect effect of ACh alone that was suitable for in vivo study at present. Further studies are required to directly examine the effect of background sympathetic tone on the direct effect of ACh through the K_{ACh} channels.

In conclusion, concomitant CSS affected no parameters of rapidity (i.e., the corner frequency in the frequency domain and the time constant in the time domain) of vagal HR control via K_{ACh} channels. Moreover, HR reduction in response to vagal stimulation via K_{ACh} channels was augmented by concomitant sympathetic stimulation at 5 Hz vagal stimulation. These findings suggest that the rapidity of response of the vagal HR control via K_{ACh} channels is invariant with respect to background sympathetic tone, and that the magnitude of vagal HR control via K_{ACh} channels is affected by background sympathetic tone in vivo.

This study was supported by Health and Labour Sciences Research Grants H15-Physi-001, H18-Nano-Ippan-003, and H18-Iryo-Ippan-023 from the Ministry of Health, Grants-in-Aid for Scientific Research promoted by the Ministry of Education, Culture, Sports, Science and Technology in Japan 18591992, 19700559, and by the Ground-based Research Announcement for Space Utilization project promoted by the Japan Space Forum. This study was also supported by an Industrial Technology Research Grant Program in 06B44524a from the New Energy and Industrial Technology Development Organization of Japan.

REFERENCES

1. Luetje CW, Tietje KM, Christian JL, Nathanson NM. Differential tissue expression and developmental regulation of guanine nucleotide binding regulatory proteins and their messenger RNAs in rat heart. J Biol Chem. 1988;263:13357-65.
2. Sunahara RK, Dessauer CW, Gilman AG. Complexity and diversity of mammalian adenylyl cyclases. Annu Rev Pharmacol Toxicol. 1996;36:461-80.
3. Huang CL, Slesinger PA, Casey PJ, Jan YN, Jan LY. Evidence that direct binding of G beta gamma to the GIRK1 G protein-gated inwardly rectifying K+ channel is important for channel activation. Neuron. 1995;15:1133-43.
4. Sakmann B, Noma A, Trautwein W. Acetylcholine activation of single muscarinic K+ channels in isolated pacemaker cells of the mammalian heart. Nature. 1983;303:250-3.
5. Yamada M, Inanobe A, Kurachi Y. G protein regulation of potassium ion channels. Pharmacol Rev. 1998;50:723-60.
6. Mizuno M, Kamiya A, Kawada T, Miyamoto T, Shimizu S, Sugimachi M. Muscarinic potassium channels augment dynamic and static heart rate responses to vagal stimulation. Am J Physiol Heart Circ Physiol. 2007;293:H1564-70.
7. Negrão CE, Rondon MU, Tinucci T, Alves MJ, Roveda F, Braga AM, Reis SF, Nastari L, Barretto AC, Krieger EM, Middlekauff HR. Abnormal neurovascular control during exercise is linked to heart failure severity. Am J Physiol Heart Circ Physiol. 2001;280:H1286-92.
8. Mancia G, Grassi G, Giannattasio C, Seravalle G. Sympathetic activation in the pathogenesis of hypertension and progression of organ damage. Hypertension. 1999;34:724-8.
9. Seals DR, Bell C. Chronic sympathetic activation: consequence and cause of age-associated obesity? Diabetes. 2004;53:276-84.
10. Hartzell HC, Méry PF, Fischmeister R, Szabo G. Sympathetic regulation of cardiac calcium current is due exclusively to cAMP-dependent phosphorylation. Nature. 1991;351:573-6.
11. Irisawa H, Brown HF, Giles W. Cardiac pacemaking in the sinoatrial node. Physiol Rev. 1993;73:197-227.
12. Breitwieser GE, Szabo G. Uncoupling of cardiac muscarinic and beta-adrenergic receptors from ion channels by a guanine nucleotide analogue. Nature. 1985;317:538-40.
13. Levy MN. Sympathetic-parasympathetic interactions in the heart. Circ Res. 1971;29:437-45.
14. Kawada T, Ikeda Y, Sugimachi M, Shishido T, Kawaguchi O, Yamazaki T, Alexander J Jr, Sunagawa K. Bidirectional augmentation of heart rate regulation by autonomic nervous system in rabbits. Am J Physiol. 1996;271:H288-95.
15. Kawada T, Uemura K, Kashihara K, Jin Y, Li M, Zheng C, Sugimachi M, Sunagawa K. Uniformity in dynamic baroreflex regulation of left and right cardiac sympathetic nerve activities. Am J Physiol Regul Integr Comp Physiol. 2003;284:R1506-12.
16. Brigham E. FFT transform applications. In: The Fast Fourier Transform and its applications. Englewood Cliffs, NJ: Prentice Hall; 1988. p. 167-203.
17. Bendat J, Piersol A. Single-input/output relationships. In: Random data: analysis and measurement procedures (3rd edition). New York: Wiley; 2000. p. 189-217.
18. Marmarelis P, Marmarelis V. The white noise method in system identification. In: Analysis of physiological systems. New York: Plenum; 1978. p. 131-221.
19. Lavine N, Ethier N, Oak JN, Pei L, Liu F, Trieu P, Rebois RV, Bouvier M, Hebert TE, Van Tol HH. G protein-coupled receptors form stable complexes with inwardly rectifying potassium channels and adenylyl cyclase. J Biol Chem. 2002;277:46010-9.
20. Nikolov EN, Ivanova-Nikolova TT. Coordination of membrane excitability through a GIRK1 signaling complex in the atria. J Biol Chem. 2004;279:23630-6.
21. Kim D. Beta-adrenergic regulation of the muscarinic-gated K+ channel via cyclic AMP-dependent protein kinase in atrial cells. Circ Res. 1990;67:1292-8.
22. Müllner C, Vorobiov D, Bera AK, Uezono Y, Yakubovich D, Frohnwieser-Steinecker B, Dascal N, Schreibmayer W. Heterologous facilitation of G protein-activated K(+) channels by beta-adrenergic stimulation via cAMP-dependent protein kinase. J Gen Physiol. 2000;115:547-58.

30th Annual International IEEE EMBS Conference
Vancouver, British Columbia, Canada, August 20-24, 2008

Modification of Autonomic Balance by Electrical Acupuncture does not Affect Baroreflex Dynamic Characteristics

Masaru Sugimachi, *Member, IEEE*, Toru Kawada,
Hiromi Yamamoto, Atsunori Kamiya,
Tadayoshi Miyamoto, and Kenji Sunagawa, *Member, IEEE*

Abstract— *Background:* **We have demonstrated that modification of autonomic balance by electrical vagal stimulation delays progression of cardiac dysfunction and cardiac remodeling, and prolongs survival in rats with severe heart failure. We have also shown that we were able to modify autonomic balance by electrical acupuncture at the acupoint of Zusanli, potentially applicable for the treatment of heart failure. We examined the effect of the acupuncture on the dynamic characteristics of the baroreflex system to exclude the possible deleterious effect on orthostatic tolerance.**

Method: **In anesthetized 8 and 6 rabbits, we examined static and dynamic characteristics of baroreflex, respectively, with and without electrical acupuncture (1 Hz, 5 mA, and 5msec). Dynamic characteristics were examined by imposing pseudorandom binary changes in isolated carotid sinus pressure.**

Results: **With the stimulation condition to decrease arterial blood pressure and sympathetic nerve activity (resulted form decreased response range of neural arc), either of the dynamic characteristics of neural arc or those of peripheral arc did not change by electrical acupuncture at Zusanli.**

Conclusion: **We conclude that application of electrical acupuncture at Zusanli can suppress sympathetic nerve activity but does not affect the dynamic characteristics of the arterial baroreflex system, indicating no deleterious effect on orthostatic tolerance.**

Manuscript received April 7, 2008. This work was supported in part by Health and Labour Sciences Research Grants (H19-nano-ippan-009, H15-physi-001) from the Ministry of Health Labour and Welfare of Japan, and by the Program for Promotion of Fundamental Studies in Health Science of the National Institute of Biomedical Innovation.

M. Sugimachi, D. Michikami, T. Kawada, H. Yamamoto, and A. Kamiya are with the National Cardiovascular Center Research Institute, Suita, Osaka 5658565, Japan (corresponding author Masaru Sugimachi to provide phone: +81-6-6833-512; fax: +81-6-6835-5403; e-mail: su91mach@ri.ncvc.go.jp).

D. Michikami is supported by a postdoctoral program by Japan Association for the Advancement of Medical Equipment.

T. Miyamoto is with Morinomiya University of Medical Sciences, Osaka 5590034 Japan. (e-mail: miyamoto@morinomiya-u.ac.jp).

K. Sunagawa is with Kyushu University Graduate School of Medical Sciences, Fukuoka 8128582 Japan. (e-mail: sunagawa@cardiol.med.kyushu-u.ac.jp).

I. INTRODUCTION

It is widely accepted that chronic heart failure involves not only abnormal structural and functional changes of heart and vessels themselves, but also abnormal changes in cardiovascular regulation. The fact that all successful cardiovascular drugs (ACE inhibitors, beta-adrenergic blockers, angiotensin receptor blockers, and aldosterone inhibitors) recently developed to treat heart failure are aimed at antagonizing neurohumoral activation has supported this.

We have shown that modification of autonomic balance by direct electrical vagal stimulation has inhibited cardiac remodeling, further deterioration of cardiac function, and improved survival in rat model of post-infarction severe chronic heart failure [1]. Because of the poor prognosis of chronic heart failure even with the use of combination of medical therapy, device-based therapy and the current state-of-art therapeutic modalities, such as cardiac transplantation, artificial heart, development of an additional therapeutic strategy attacking the abnormal cardiovascular regulation seems of great value to help still unsaved patients.

We have also shown in the last meeting that we were able to modify autonomic balance by electrical acupuncture at the acupoint of Zusanli, which is potentially applicable to treat heart failure. The less invasive nature of the acupuncture would greatly enhance its widespread use.

In this article, we have examined the effect of the acupuncture on the dynamic characteristics of the baroreflex system to ensure that there is no deleterious effect on orthostatic tolerance. The results indicated that electrical acupuncture is able to suppress sympathetic nerve activity but does not affect the dynamic characteristics of the arterial baroreflex system.

II. MODEL AND METHODS

A. Animal Experiments

We used 8 rabbits (Japanese White) to examine the effects of electrical acupuncture on open-loop static characteristics of baroreflex system. The effects of electrical acupuncture on open-loop dynamic characteristics were examined in other 6 rabbits.

978-1-4244-1815-2/08/$25.00 ©2008 IEEE.

In both protocols, rabbits were cared for in accordance with the Guiding Principles for the Care and Use of Animals in the Field of Physiological Sciences approved by the Physiological Society of Japan. These animals were anesthetized by a mixture of urethane (250 mg/ml) and α-chloralose (40 mg/ml) with an initial dose of 2 ml/kg (iv) and additional doses to maintain an appropriate level of anesthesia. Rabbits were mechanically ventilated with oxygen-enriched room air. Pancuronium bromide (0.1 mg/kg), a muscle relaxant was administered to prevent contaminating muscular activities.

A catheter-tipped micromanometer was inserted into a femoral artery to measure arterial blood pressure. After thoracotomy, we identified a left cardiac sympathetic nerve and the peripheral end was cut. Its efferent activity was recorded by a pair of stainless steel wire electrodes attached to the central end. We used silicone glue (Kwik-Sil, World Precision Instruments, Sarasota, FL) to fix the electrode, to provide insulation and to prevent the nerve from drying. We band-pass filtered the electrical signal at 150–1000 Hz and full-wave rectified, and low-pass filtered at a cutoff frequency of 30 Hz to quantify nerve activity.

To open the negative feedback loop, we isolated both carotid sinuses from the systemic circulation. We filled the isolated carotid sinuses with warmed physiological saline for longer preservation of baroreflex function. The blind-sac carotid sinuses were connected to a servo-controlled piston pump (model ET-126A, Labworks, Costa Mesa, CA) to control the pressure imposed on baroreceptors. Although being unphysiological and making baroreflex gain lower, it was necessary to cut bilateral vagal nerves and bilateral aortic depressor nerves to make baroreflex system fully open-loop condition.

Signals such as arterial blood pressure (AP), integrated sympathetic nerve activity (SNA), and carotid sinus pressure (CSP) were simultaneously digitized by a 12-bit analog-to-digital converter interfaced with a laboratory computer, and were stored on a hard disk for offline analysis. We used an arbitrary unit for nerve activity.

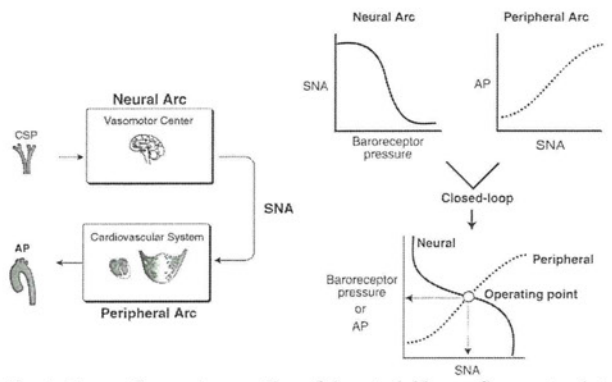

Fig. 1. Decoupling and recoupling of the arterial baroreflex system into neural arc and peripheral arc. CSP, carotid sinus pressure; AP, arterial blood pressure; SNA, sympathetic nerve activity.

B. *Method to Identify Static Open-loop Characteristics of Baroreflex System*

We have opened (see above) the total negative feedback loop of the arterial baroreflex system, and subdivided it into two subsystems. The two subsystems include the "neural arc" (which in turn includs baroreceptor and vasomotor center) and the "peripheral arc" (which in turn includes various sympathetic effectors). The neural arc corresponds to the controller and the peripheral arc corresponds to the plant of the baroreflex feedback system [2].

To quantify the static characteristics, we imposed stepwise change in CSP from 40 mmHg to 160mmHg with an increment of 20 mmHg. The particular CSP level was maintained for 60 seconds and the steady-state CSP, SNA, and AP were quantified by averaging the digitized values for the last 10 seconds.

We have characterized the neural arc by the relationship between CSP and SNA. We have characterized the peripheral arc by the relationship between SNA and AP. By recoupling these curves we can determine the operating point of the baroreflex system under the closed-loop condition by the intersection between the neural and peripheral arc curves.

C. *Method to Identify Dynamic Open-loop Characteristics of Baroreflex System*

We identified the dynamic characteristics of baroreflex, with or without electrical acupuncture. We imposed CSP changes around the respective closed-loop operating point with the amplitude of 20 mmHg according to a pseudorandom binary sequence.

The wideband nature of white noise input allows estimation of the wideband system dynamic properties. In addition, we ensemble-averaged the input power and cross power across multiple segments to reduce the statistical variance [3, 4].

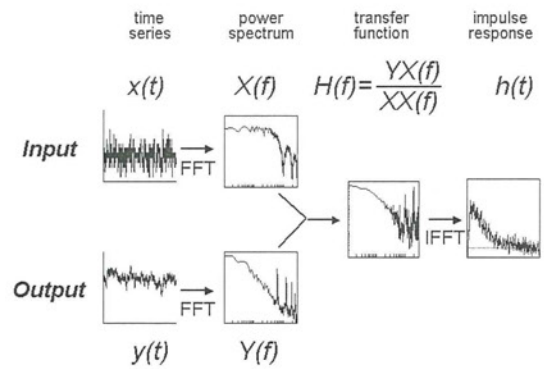

Fig. 2. Method to identify dynamic characteristics of a system. x(t), input signal; y(t), output signal; X(f) and Y(f), amplitude spectrum of x(t) and y(t), respectively; XX(f) and YX(f), ensemble-averaged input power spectrum and cross power (between input and output) spectrum, respectively; H(f), transfer function; h(t), impulse response.

We identified neural arc dynamic characteristics by analyzing CSP as input and SNA as output. We also identified peripheral arc dynamic characteristics by analyzing SNA as input and AP as output. Total baroreflex dynamic characteristics were obtained by analyzing CSP as input and AP as output.

In reference to Fig. 2, both input [x(t)] and output [y(t)] signals are divided into multiple segments. These data are subjected to frequency analysis using a fast Fourier transform (FFT) algorithm [X(f) and Y(f)]. The calculated input power and cross power (between input and output signals) are ensemble-averaged across segments to reduce variance [XX(f) and YX(f)]. Finally the transfer function [H(f)] is obtained by dividing the ensembled cross power by the ensembled input power. The impulse response [h(t)] is calculated by the inverse FFT of the transfer function.

D. *Electrical Acupuncture*

We have performed electrical acupuncture at Zusanli, i.e., the one-fifth point (from the knee) with the use of a pair of stainless steel wires (0.2 mm in diameter). The midpoint of the knee-ankle distance of approximately 30–35 mm served as the reference electrode. These needles were inserted to a depth of 10 mm in the skin and underlying muscle (the tibialis anterior muscle) [5].

The effects of Zusanli stimulation on baroreflex neural and peripheral arc characteristics were studied with the stimulation condition of 1 Hz, 5 mA, and 5msec. The stimulation condition is based on preliminary experiments.

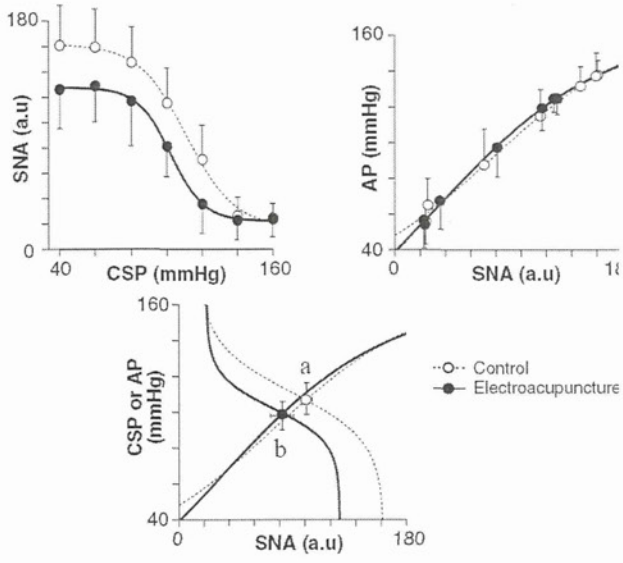

Fig. 3. Effect of electrical acupuncture on neural arc (top left) and peripheral arc (top right) static characteristics of arterial baroreflex, superimposed neural and peripheral arc curves (bottom). CSP, carotid sinus pressure; AP, arterial blood pressure; SNA, sympathetic nerve activity; solid line, with electrical acupuncture; dashed line, without electrical acupuncture, error bars, 1SD.

III. Results

A. *Effects on Static Characteristic*

The response range of SNA for the CSP change of 40-160 mmHg was obviously decreased with Zusanli stimulation (neural arc, Fig. 3 top left). The peripheral arc does not seem to change by Zusanli stimulation (Fig. 3 top right). These changes resulted in the decreased AP and SNA at the closed-loop operation point (Fig. 3 bottom).

B. *Effects on Dynamic Characteristic*

Fig. 4 exemplifies the time series of data obtained before and during pseudorandom changes in CSP. We imposed changes in CSP of ±20 mmHg around the respective closed-loop operating point.

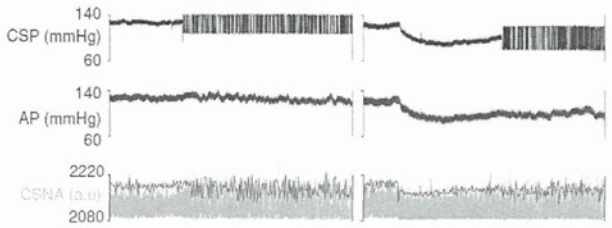

Fig. 4. An example of time series before and during changes in carotid sinus pressure according to pseudorandom binary sequence, with (right) and without (left) electrical acupuncture. CSP, carotid sinus pressure; AP, arterial blood pressure; CSNA, cardiac sympathetic nerve activity.

Changes in dynamic characteristics of neural arc, peripheral arc, and total loop by electrical acupuncture are shown in Fig. 5. As shown in the figure, transfer functions (dynamic characteristics) of neural arc, peripheral arc, and total loop were superimposable.

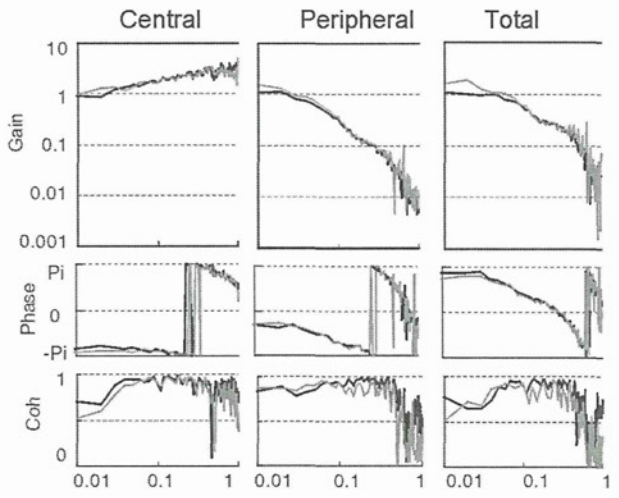

Fig. 5. Transfer functions (dynamic characteristics) of neural arc (left), peripheral arc (middle), and total loop (right) of baroreflex, with (gray) and without (black) electrical acupuncture. From top to bottom, gain, phase, and squared magnitude of coherence are shown.

IV. Discussion

We have repeatedly demonstrated that electrical vagal stimulation was successful in retarding further deterioration of cardiac function and progression of cardiac remodeling in rats with severe heart failure. This therapeutic method is also capable of prolonging survival in heart failure rats. These effects were believed to be mediated by the modification of autonomic balance.

Based on these results, several groups of investigators are developing an implantable vagal neurostimulators to apply this method for the human use; the invasive nature of the implantable device is likely to limit its widespread use, especially in relatively mild cases of heart failure.

A less invasive measure is definitely needed. To develop a less invasive method for modifying autonomic balance, we have examined the effect of Zusanli electrical stimulation. This method has been used to treat various diseases in oriental medicine.

To ensure these effects of traditional medicine, we have conducted animal experiments. The results have shown depressor and sympathetic neuroinhibitory (static) effect during Zusanli electrical stimulation. These effects are mediated by the changes in neural arc. We have also demonstrated that dynamic characteristics of baroreflex neural and peripheral arcs did not change by Zusanli electrical stimulation. We conclude that application of electrical acupuncture can suppress sympathetic nerve activity but does not affect the dynamic characteristics of the arterial baroreflex system, indicating no deleterious effect on orthostatic tolerance.

References

[1] M. Li, C. Zheng, T. Sato, T. Kawada, M. Sugimachi, K. Sunagawa. "Vagal nerve stimulation markedly improves long-term survival after chronic heart failure in rats." *Circulation.* Vol. 109, pp. 120-124, Jan. 2004.

[2] T. Sato, T. Kawada, M. Inagaki, T. Shishido, H. Takaki, M. Sugimachi, K. Sunagawa, "New analytic framework for understanding sympathetic baroreflex control of arterial pressure." *Am. J. Physiol. Heart Circ Physiol.* vol. 276, no. 6, pp. H2251-H2261, Jun. 1999.

[3] P. Z. Marmarelis and V. Z. Marmarelis, Analysis of Physiological Systems: The White-Noise Approach, New York, NY: Plenum, 1978.

[4] J. S. Bendat, and A. G. Piersol, Random Data: Analysis & Measurement Procedures, 3rd Ed., New York, NY: Wiley-Interscience, 2000

[5] D. Michikami, A. Kamiya, T. Kawada, M. Inagaki, T. Shishido, K. Yamamoto, H. Ariumi, S. Iwase, J. Sugenoya, K. Sunagawa, M. Sugimachi. "Short-term electroacupuncture at Zusanli resets the arterial baroreflex neural arc toward lower sympathetic nerve activity." *Am J Physiol Heart Circ Physiol.* vol. 291, pp. H318-H326, Jul. 2006.

Autonomic Neuroscience: Basic and Clinical 144 (2008) 43–49

Contents lists available at ScienceDirect

Autonomic Neuroscience: Basic and Clinical

journal homepage: www.elsevier.com/locate/autneu

Electroacupuncture changes the relationship between cardiac and renal sympathetic nerve activities in anesthetized cats

Hiromi Yamamoto [a,*], Toru Kawada [b], Atsunori Kamiya [b], Toru Kita [a], Masaru Sugimachi [b]

[a] Department of Cardiovascular Medicine, Graduate School of Medicine, Kyoto University, Kyoto 606-8501, Japan
[b] Department of Cardiovascular Dynamics, Advanced Medical Engineering Center, National Cardiovascular Center Research Institute, Osaka 565-8565, Japan

ARTICLE INFO

Article history:
Received 5 June 2008
Received in revised form 13 August 2008
Accepted 12 September 2008

Keywords:
Hind limb stimulation
Baroreflex
Arterial blood pressure
Heart rate

ABSTRACT

Electroacupuncture (EA) is known to affect hemodynamics through modulation of efferent sympathetic nerve activity (SNA), however, possible regional differences in the SNA response to EA remains to be examined. Based on the discordance between arterial blood pressure and heart rate changes during EA, we hypothesized that regional differences would occur among SNAs during EA. To test this hypothesis, we compared changes in cardiac and renal SNAs in response to 1-min EA (10 Hz or 2 Hz) of a hind limb in adult cats anesthetized with pentobarbital sodium. Renal SNA remained decreased for 1 min during EA ($P<0.01$ for both 10 Hz and 2 Hz). In contrast, cardiac SNA tented to decrease only in the beginning of EA. It increased during the end of EA ($P<0.05$ for 2 Hz) and further increased after the end of EA ($P<0.01$ both for 10 Hz and 2 Hz). There was a quasi-linear relationship between renal and cardiac SNAs with a slope of 0.69 (i.e., renal SNA was more suppressed than cardiac SNA) during the last 10 s of EA. The discrepancy between the renal and cardiac SNAs persisted after sinoaortic denervation and vagotomy. In conclusion, EA evokes differential patterns of SNA responses and changes the relationship between cardiac and renal SNAs.

1. Introduction

Electroacupuncture stimulation has been used to modulate autonomic nervous activity and cardiovascular function (Kimura and Sato, 1997; Lin et al., 2001). Several studies have demonstrated that arterial blood pressure (AP) is decreased by acupuncture-like stimulation in anesthetized animals (Kline et al., 1978; Ku and Zou, 1993; Lee and Kim, 1994; Zhou et al., 2005). The cardiovascular responses induced by acupuncture-like stimulation are reflexes mediated via somatic afferent nerves and autonomic efferent nerves (Sato et al., 1994, 2002). Although slow-onset, long-lasting effects may be characteristics of acupuncture, rapid-onset, short-lasting effects are also reported in some experimental conditions. In anesthetized rats, Ohsawa et al. (1995) reported that acupuncture-like stimulation of a hind limb decreased AP in association with a decrease in renal sympathetic nerve activity (RSNA). Uchida et al. (2007) reported that acupuncture-like stimulation of a hind limb induced decreases in cardiac sympathetic nerve activity (CSNA) and heart rate (HR). On the other hand, Kobayashi et al. (1998) reported that acupuncture stimulation produced variable responses including tachycardia, bradycardia, or no responses. We hypothesized that regional differences in sympathetic nerve activities would account for the diverse HR response and more consistent hypotensive response reported during EA. Although Sato et al. (1981) reported that stimulation of group III muscle afferent fibers of a hind limb induces either bradycardic or tachycardic response in anesthetized cats, they did not measure efferent sympathetic nerve activities. To test the hypothesis that EA would evoke regional differences among sympathetic efferent nerve activities, we simultaneously recorded and directly compared CSNA and RSNA during EA in anesthetized cats. The kidneys are important for a long-term AP control via the maintenance of sodium and water balance (DiBona, 2005). At the same time, because the kidneys receive approximately 20% of the cardiac output in resting humans (Rowell, 1974), we thought changes in RSNA could contribute to the acute AP control. We first examined changes in AP, HR, CSNA, and RSNA in response to 10-Hz or 2-Hz EA of a hind limb. We then investigated possible roles of arterial baroreflex and vagal nerve activities in the effects of EA using sinoaortic denervation and vagotomy.

2. Methods

2.1. Surgical preparation

Animal care was provided in strict accordance with the Guiding Principles for the Care and Use of Animals in the Field of Physiological Sciences approved by the Physiological Society of Japan. All protocols were approved by the Animal Subject Committee of National Cardiovascular Center. Adult cats weighing 3.0 to 5.2 kg were anesthetized by an intraperitoneal injection of pentobarbital sodium (30–35 mg/kg) and ventilated mechanically via a tracheal tube with oxygen-supplied room air. The depth of anesthesia was maintained with a continuous intravenous infusion of pentobarbital sodium (1–2 $mg \cdot kg^{-1} \cdot h^{-1}$) through a catheter inserted into the right femoral vein. Vecuronium bromide (0.5–

* Corresponding author. Tel.: +81 75 751 3195; fax: +81 75 751 3203.
E-mail address: hiromi@kuhp.kyoto-u.ac.jp (H. Yamamoto).

1566-0702/$ – see front matter © 2008 Elsevier B.V. All rights reserved.
doi:10.1016/j.autneu.2008.09.002